Integration of acoustic constraints in trajectory generation

Damien Hoareau[1], Danil Berrah[1], Joris Tillet[1] and Alexandre Chapoutot[1]

***Abstract*— Optimal control based trajectory generation offers the ability to formulate complex problems while optimizing the performance of the system control inputs. Nevertheless, adding acoustic constraints to the optimal control problem (OCP) can be highly challenging. The classical resolution approach employs a "first-discretize-then-optimize" strategy using direct methods. However, this approach leads to significant computational costs, which in turn limits its applicability. Recent studies suggest using the acoustic reciprocity theorem (ART) to formulate the problem as one of obstacles collision avoidance. Hence, this study proposes investigating the formulation and solution of an OCP based on this theorem. The ART is combined with the Boundary Element Method (BEM) for the acoustic part of the problem. The OCP is implemented using successive convexification (SCvx) approach which offers a convenient framework to take into account acoustic constraint in trajectory planning generation. Promising experimental results highlight the applicability of our formulation based on the ART and guidelines for further development are provided.**

I. INTRODUCTION

In recent decades, autonomous robot navigation has attracted significant interest and has become a widely studied field. There are several areas of application, such as industry, agriculture, the military or transportation. Among the different issues covered, path planning or trajectory generation can be found as the most common [1]. Well-known algorithms and methods can be found in the literature [2], each with its own characteristic. Nevertheless, increasing development of new technologies brings not only new opportunities but also challenges. Indeed, to meet the needs in terms of efficiency, complex nonlinear systems including physical constraints have emerged. Therefore, new solutions based on optimal control such as *model predictive control* (MPC) method are being adopted across the board [3]. This allows to solve the problem of path planning by taking into account complex physical limitations while improving control performances.

a) Problem Definition: The typical objectives of trajectory generation is to find the shortest path and avoid collision. However, with the proliferation of robotic systems, especially drones, acoustic compliance and noise limitations have garnered significant attention. Indeed, discretion of the systems is crucial for logistic operations, filming in urban environments or for security mission. Thus, silent path planning or paths with limited acoustic signatures are becoming key considerations.

This work was supported by *Agence de l'Innovation de Défense* – AID – via *Centre Interdisciplinaire d'Études pour la Défense et la Sécurité* – CIEDS – (project – APRO)

[1]D. Hoareau, D. Berrah, J. Tillet and A. Chapoutot are with the Computer Science and Systems Engineering Laboratory (U2IS), ENSTA, Institut Polytechnique de Paris, 91120 Palaiseau, France {hoareau,berrah,tillet,chapoutot}@ensta.fr

Yet, the resolution of such a problem is hard. The general formulation of the *optimal control problem* (OCP) including acoustic constraints can be expressed as

$$\min_{x(t),u(t)} \quad \int_{t_0}^{t_f} L(x(t),u(t),t)\,dt + \varphi(x(t_f),u(t_f)) \tag{1a}$$

subject to

$$\dot{x}(t) = f(x(t),u(t)), \tag{1b}$$

$$h_i(x(t),u(t)) \leq 0, \quad i \in [1,n], \tag{1c}$$

$$g_j(x(t),u(t)) = 0, \quad j \in [1,m], \tag{1d}$$

$$\frac{\partial^2 p(t,x(t))}{\partial t^2} - c^2\nabla^2 p(t,x(t)) = s(x(t),u(t)) \in \mathbb{R}^k \setminus \Omega, \tag{1e}$$

$$p(t,x_\ell(t)) \leq \xi_l, \quad \ell \in [1,q], \tag{1f}$$

$$x \in \mathcal{X} \subseteq \mathbb{R}^{n_x}, \quad u \in \mathcal{U} \subseteq \mathbb{R}^{n_u}, \quad t \in [t_0,t_f].$$

The objective function to minimize (1a) is expressed in the generic Bolza form. Equation (1b) represents the system dynamics. The terms $x(\cdot)$ and $u(\cdot)$ refer to the system states and control inputs, respectively. Equations (1c) and (1d) represent the system states constraints and control constraints. Equation (1e) stands for the propagation of the sound pressure in the considered media $\mathbb{R}^k \setminus \Omega$, where Ω is the space of existing static obstacles. The term $s(\cdot,\cdot)$ is the acoustic source term, which depends on the system dynamics and Equation (1f) is the acoustic pressure constraints.

The resulting coupled *ordinary differential equation* (ODE) and hyperbolic *partial differential equation* (PDE), involving the states and control inputs constraints, make solving the problem very complex. State-of-the-art *first-discretize-then-optimize* approaches are frequently used for this kind of problem [4]. Direct methods based on sequential quadratic programming (SQP) [5] algorithms or nonlinear programming solvers are suggested [6]. Nonetheless, despite the inherent complexity and significant computational demands, challenges begin by emerging from dimension $k = 2$.

Hopefully, approximations and reformulations of the general Problem (1) may provide alternative solutions, depending on the desired performance. In the following, we provide an overview of the currently employed approaches, their limitations, and the overall structure of the paper.

b) Related Work: In this overview, a differentiation is made between sound propagation with and without scattering. Sound scattering refers to the reflection and diffusion of sound due to obstacles.

Path planning with long-distance sound propagation typically focuses on the effects of the ground and wind (*e.g.*,

aircraft trajectory generation, high-altitude flight). Most of the time, there are direct acoustic paths between the acoustic source and the observers, leading to explicit sound estimation [7]–[10]. Ackerman *et al.* [11] incorporated explicit sound estimation into a planner based on Bézier curves and MPC. Moreover, in other scenarios it can be sufficient to use simpler model. Adlakha *et al.* [12] present in their study an acoustic-infused path planning framework. They used the $A*$ algorithm and infused an acoustic cost based on their acoustic model. The sound scattering was not modeled but can be added by using higher fidelity models as suggested by the authors.

Ensuring the non violation of acoustic constraints integrating high fidelity models may be complicated. Computational efficiency, algorithm performance and variables optimization can be seen as key features in path planner. Hence, the estimation of the sound propagation must be efficient. Some of the methods available for computing sound pressure field include, but are not limited to, *finite element method* (FEM) [13], *finite difference methods* (FDMs) [14], *boundary element method* (BEM) [15], ray tracing method [16] and deep learning approaches [17]. The BEM demonstrates better applicability for large-scale problems (*e.g.*, exterior problems) and provides precise modeling of scattering phenomena. However, complex geometry scenarios increase its numerical cost. Ray tracing methods offer strong computational efficiency but struggle to accurately model complex wave phenomena such as diffusion. The FDM is well suited for time-domain simulation with very simple geometry. FEMs are capable of handling intricate geometries, but are highly sensitive to mesh size, which significantly affects accuracy and computational needs. Deep learning approaches enable faster simulations of complex scenarios but often suffer from a lack of generalization and remain difficult for outdoor environments.

Furthermore, optimal control based algorithms require multiple functions computations. As a result, repeatedly evaluating sound propagation can become computationally inefficient when combined with an optimization solver. Gao *et al.* [18] suggest in their study to develop a virtual acoustic terrain using the *acoustic reciprocity theorem* (ART) [19]–[21]. The acoustic reciprocity principle states that the receiver and the source can be swapped without modification of the amplitude and phase of the measured acoustic pressure field. The ART is applicable to linear-elastic medium such as air at rest [22]. Hence, exclusion zones can be generated from the receiver locations using the source characteristics, bounded by the maximum acceptable acoustic noise level. The problem is reduced to collision avoidance within the excluded zones associated to zones where the acoustic level should not be crossed.

c) Contribution: To the best of our knowledge, studies are often limited to the trajectory generation with acoustic constraints without scattering. Thus special attention is given to this aspect as it implies supplementary considerations, especially when integrated in an OCP-based path planner. Hence, we propose a new OCP-based planner taking into account acoustic constraint. Note that our proposed approach is generic as it does not rely on a specific acoustic model which usually depends on a particular application.

The BEM seems to be a good candidate for modeling the scattering phenomena. Thus, the current paper focuses on the integration of acoustic constraints in the path planning framework using BEM. The General Problem (1) is mostly solved using SQP algorithms based on large-scale nonlinear solver. Nonetheless, recent studies proposed convex optimization-based algorithms relying on linearization and convexification of the original problem. This ensures polynomial-time complexity while guaranteeing convergence. In [23], a study on *Successive Convexification* (SCvx) algorithm is presented, where multiple convex sub-problems are successively solved.

In order to reduce the numerical cost due to repetitive evaluation of sound propagation in the solver, the ART-based approach is used to build exclusion zones. Virtual obstacles are extracted and are formulated as non-collision constraints, the externalized acoustic computations are performed in the optimization framework. Hence, the current study adopts the SCvx algorithm to demonstrate the integration of the BEM into an OCP-based planner as part of an efficient reformulation.

d) Contents: The following sections are structured as follows: an overview of the BEM and SCvx algorithm is provided in Section II; the reformulated Problem (1) and an example under consideration are presented in Section III; in Section IV the main results are introduced and the key ideas are highlighted; finally, Sections V and VI conclude the study with a discussion and future work.

II. BACKGROUND

A. Boundary Element Method

Linear PDE formulated as integral equations can be solved numerically using the BEM [24]. The boundary integral form gives the exact solution to the governing equations which is determined entirely by the boundary conditions and values. In acoustics, the time-dependent scalar wave equation, Equation (2), can be transformed into homogeneous Helmholtz equation, Equation (3), by using the Laplace operator

$$\frac{\partial^2 u}{\partial t^2} = c^2 \nabla^2 u, \tag{2}$$

and

$$k^2 u + \nabla^2 u = 0, \tag{3}$$

where k is the wave number and c is the speed of sound, u is the acoustic pressure, t is the time. Then the considered problem is constructed using boundary integral operators, depending on the problem, such as the single layer operator, Equation (4), or double layer operator, Equation (5):

$$p, q \mapsto \mathcal{SL}(p, q) = \int_{\Gamma \times \Gamma} p(x)\, q(y)\, G_k(x - y)\, d\sigma(x, y), \tag{4}$$

and

$$p, q \mapsto \mathcal{DL}(p,q) = \int_{\Gamma\times\Gamma} p(x)\, q(y)\, \frac{\partial}{\partial n(y)} G_k(x-y)\, d\sigma(x,y), \quad (5)$$

where Γ is the boundary of the domain in which sound wave evolves and x is the position of the observation point, y is the position of the acoustic source, p and q are functions, n is the outgoing boundary normal and $d\sigma$ is the integration element on the boundary of the domain. The Green kernel $\mathcal{G}_k$ for Helmotz equation is

$$\mathcal{G}_k = \frac{i}{4} H_0^{(1)}(k|x|), \quad \text{in 2D}, \quad (6)$$

and

$$\mathcal{G}_k = \frac{\exp(ik|x|)}{4\pi|x|}, \quad \text{in 3D}, \quad (7)$$

where $H_0^{(1)}$ denotes the Hankel function of the first kind. There are other operators that can also be used either alone or in combination with others, depending on the choice of the problem formulation. Finally, the solution is obtained by formulating a variational problem with an associated test function and performing integration over the boundaries.

In this study, computations are performed under the *Bempp* [25] framework, an open-source Python package for BEM which has an efficient implementation of operators given in Equation (4) and Equation (5).

B. Successive convexification

The SCvx algorithm is part of *sequential convex programming* (SCP) methods. The original problem is convexified sequentially by linearizing the nonconvexities. Then, the created convex sub-problem is temporally discretized. The discretization can be performed using a *first-order hold* (FOH) interpolation method, for example. Due to the linearization process, artificial infeasability and unboundedness artifacts are introduced. This is handled by the augmentation of the linearized equations by adding virtual control terms and a trust region. At each convexification sequence or iteration, the convex sub-problem is solved using a convex optimizer and the obtained solution is used to adapt SCvx algorithm parameters. The stopping criterion is globally based on the difference between the current iteration trajectory solution and the previous one. A low value means that there will be no further improvements in future iterations. A brief description of the algorithm is provided in Algorithm 1.

Algorithm 1 Successive Convexification

```
Input: Initial discretized trajectory i = 1...N
Output: Optimized discretized trajectory i = 1...N
Initialize variables
for iteration k = 1 to MaxIterations do
    Linearize nonconvexities
    Temporally discretize
    while Local solution not accepted do
        Solve convex sub-problem
        if Converged then
            Stop algorithm
            Return result
        else
            Handle intrinsic artifacts
            Update initial trajectory to current trajectory
        end if
    end while
end for
```

The problem is initially linearized around the initial trajectory. If the convergence criterion is not met, a new solution is generated and used for the subsequent linearization process. The reader is referred to [26] for further explanations of the SCvx algorithm. Existing implementation of the SCvx algorithm can be found at `https://github.com/EmbersArc/SCvx.git` and served as a basis for development in this paper.

III. MATERIALS AND METHODS

The focus is not on the linearization and discretization processes, as these are well-documented in the literature. Instead, the emphasis is placed on the integration and implementation of the acoustic part in the OCP.

A. Reformulated optimal control problem

As aforementioned, using the ART, acoustic constraints can be represented as exclusion zones. Hence, the original Problem (1) can be reduced to a path planning problem with non-collision constraints. The obstacles to be avoided are real physical obstacles and virtual obstacles constructed from the acoustic exclusion zones.

Based on the SCvx algorithm paradigm, virtual obstacles computations can be integrated in the convexification sequence using BEM. Virtual obstacles shapes are updated at each sequence iteration k for each discretization point i according to the trajectory. The controls are assumed to be piece-wise constant, thus, steady state of sound propagation is considered for each discretized time interval. The algorithm can be adapted to the new form presented in Algorithm 2.

SCvx algorithm offers a convenient basis to embed the BEM algorithm without unnecessarily loading the convex solver.

B. Models

In the current study, the differential drive robot (Dubin's car) model is considered as an example. Its dynamics can be expressed as:

$$\dot{x} = u_1 \cos(\theta), \quad \dot{y} = u_1 \sin(\theta), \quad \dot{\theta} = u_2, \quad (8)$$

where $X = [x, y, \theta]$ represents the states and $U = [u_1, u_2]$ denotes the input controls.

The associated acoustic model is defined by a monopole source given by:

$$p(r) = B_0 \frac{e^{ikr}}{r}, \quad (9)$$

where $p(\cdot)$ denotes the acoustic pressure, B_0 represents the source amplitude, $k = \frac{\omega}{c}$ is the wave number, c is the speed of sound and r is the distance from the source to the receiver. For convenience, the sound pressure level (SPL) is used for measuring the emitted noise, Eq. (10):

$$L_p = 20\log(\frac{p_{\text{rms}}}{p_{\text{ref}}}), \tag{10}$$

where $p_{\text{ref}} = 2e^{-5}$ Pa is the reference sound pressure and p_{rms} is the *root mean square* of the sound pressure.

The coupling between the system dynamics and acoustics is obtained through the equations system, Eq. (11),

$$\begin{cases} \omega = 2\pi 100(1+u_1) \\ B_0 = 0.4 + 0.05u_1 \end{cases}. \tag{11}$$

The parameters are without a particular physical meaning.

C. The acoustic problem

At each receiver location j the following exterior acoustic problem is solved, Eq. (12)

$$\begin{cases} \Delta u + k^2 u = 0, \quad \text{in } \mathbb{R}^2 \setminus \Omega, \\ u = -p_i^k \quad \text{on } \Gamma, \\ \lim_{|x|\to\infty} |x| \left(\frac{\partial}{\partial |x|} - ik\right) u(x) = 0, \end{cases} \tag{12}$$

where Ω is the physical obstacle, Γ the boundary of Ω and p is the incident acoustic wave defined in Eq. (9). The total acoustic pressure is defined as $u_{\text{tot}} = u + p$. The Dirichlet boundary condition is considered. The last equation in Eq. (12) represents the Sommerfeld radiation condition at infinity, ensuring that only outgoing waves are present at infinity. The solution u to the Helmholtz equation can be solved using the single layer potential expressed as

$$u(x) = \int_\Gamma \mathcal{G}_k(x-y)v(y)d\sigma(y), \quad \forall x \in \mathbb{R}^n \setminus \Omega, \tag{13}$$

Algorithm 2 Successive Convexification - BEM

```
Input: Initial discretized trajectory i = 1...N
Output: Optimized discretized trajectory i = 1...N
Initialize variables
for iteration k = 1 to MaxIterations do
    Linearize nonconvexities
    Temporally discretize
    (+) BEM computations
    (+) Virtual obstacles updates
    while Local solution not accepted do
        Solve convex subproblem
        if Converged then
            Stop algorithm
            Return result
        else
            Handle intrinsic artifacts
            Update initial trajectory to current trajectory
        end if
    end while
end for
```

where v is the *ansatz* to be found. This can be done using the single layer operator (see Eq. (4)).

D. Virtual obstacle construction

Once the acoustic pressure field is solved, exclusion zones can be constructed according to the maximum admissible noise level. Depending on the system configuration, complex geometry of the bounded acoustic zone may arise from the scattered waves. In addition, integrating non-collision constraints with nonconvex geometries can be challenging. Various techniques exist to formulate collision avoidance constraints for such geometries. One alternative is to use convexification algorithms, such as the convex hull or a zonotopic representation [27]. This step is user-dependent and does not affect the workflow of the proposed method. In the current paper, a *quadtree* partitioning is employed to construct the virtual obstacles. This is a simple and effective method for demonstrating the implementation of the OCP reformulation. Each leaf of the *quadtree* can be associated to a generic geometry such as a circle. The number of virtual obstacles depends on the *quadtree* depth level. Fig. 1 summarizes the workflow of virtual acoustic construction using the ART.

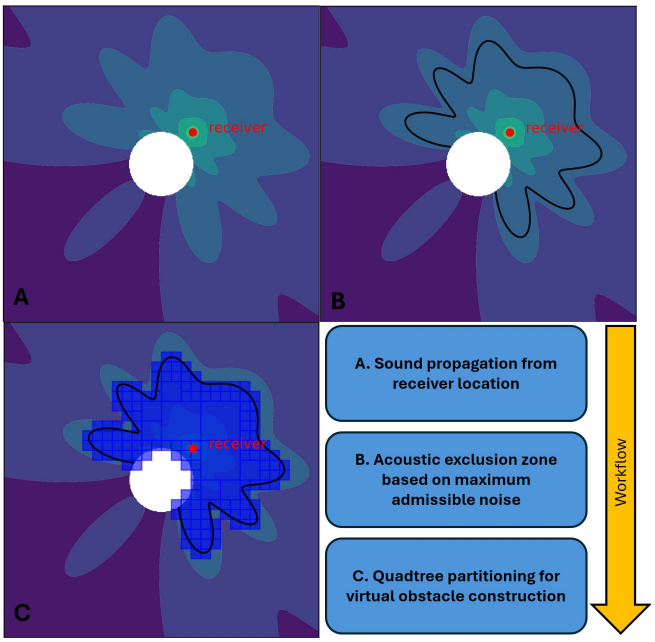

Fig. 1. Workflow of virtual obstacle construction. The white circle is an existing obstacle. The red dot is the receiver location. In A, sound propagation is calculated from the receiver location as a function of source parameters. In B, the black line represents the user-defined acoustic exclusion zone. In C, using *quadtree* partitioning, the exclusion zone is divided into multiple blocks seen as virtual obstacles.

E. Case study

The considered OCP is a fixed-time path planning problem with collision avoidance. The problem to solve in SCvx can be written in its continuous form as in Problem (14). Where ${}^{c}\cdot$ defines the cartesian coordinates of the considered parameter and P the total number of physical and virtual

obstacles. One physical obstacle is placed at ${}^{c}x_0^{\text{obs}} = [0, 0]$ with a radius equal to $r_0^{\text{obs}} = 1$. An acoustic receiver is located at $[3, 2.5]$. The exclusion zones are constructed using a maximum SPL equal to 75 dB and the *quadtree* maximum depth level is set to 6. Acoustic computations are externalized in the convexification sequence as discussed and the generated virtual obstacles are integrated in the local problem constraints. Since SCvx paradigm allows the initial trajectory to be infeasible, a simple straight-line path is chosen between the starting and ending points.

$$\min_{x(t),u(t)} \quad \int_{t_0}^{t_f} u(t)^2 dt \tag{14a}$$

subject to

$$\dot{x}(t) = f(x(t), u(t)), \tag{14b}$$

$$\|{}^{c}x(t) - {}^{c}x_n^{\text{obs}}\| \geq r_n^{\text{obs}}, \quad n \in [1, P], \tag{14c}$$

$$0 \leq u(t) \leq 1, \quad t_0 = 0, \quad tf = 25, \tag{14d}$$

$$x(0) = [-8, -8, 0], \quad x(tf) = [8, 9, 0], \tag{14e}$$

$$u(0) = [0, 0], \quad u(tf) = [0, 0], \tag{14f}$$

$$x \in \mathcal{X} \subseteq \mathbb{R}^{n_x}, \quad u \in \mathcal{U} \subseteq \mathbb{R}^{n_u}, \quad t \in [t_0, t_f],$$

IV. Results

The results can be reproduced with the codes available at `https://gitlab.ensta.fr/ssh/ocp-bem-scvx.git`. Computations were performed on **Ubuntu 20.04.6 LTS** with **Intel(R) Core(TM) i9-9900K CPU (3.60 GHz)**. To improve computational efficiency, externalized BEM computations were performed in parallel on CPU with 8 workers. Fig. 2 presents the optimal solution obtained for problem (2).

The system has avoided the physical obstacle and the acoustic exclusion zone due to sound propagation and scattering. The algorithm converged after 18 iterations. Each iteration took approximately 30 to 40 seconds to complete.

Using the ART, the SPL of the different trajectory points at the receiver location can be observed in Fig. 3.

All constraints, including the acoustic constraint, are satisfied: the system SPL remains below 75 dB at the receiver location throughout the entire trajectory. Obtained system control inputs are given in Fig. 4.

V. Discussion

The proposed OCP reformulation based on the ART gives promising results. The acoustic constraint was successfully integrated in the trajectory generation. Externalized acoustic computations using efficient solver such as BEM offer good performance for exterior and acoustic scattering problem. Repetitive evaluation of sound propagation for each discretized trajectory point is avoided as it is not directly integrated in the convex solver computations.

Nevertheless, some considerations emerge from the virtual obstacle construction. The exclusion zones may have complex shapes making obstacle avoidance formulation difficult. Space partitioning using *quadtree* allows to formulate

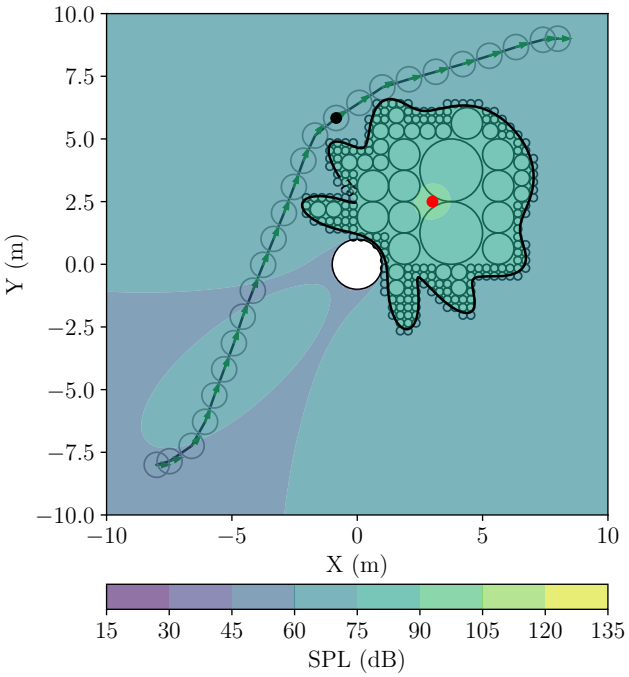

Fig. 2. Generated optimal trajectory of problem (2) with externalized BEM computations. The white circle represents the physical obstacle. The red dot represents the receiver location. The thick black line represents the acoustic exclusion zone according to the discretized trajectory point in black dot. The multiple black line circles in the exclusion zone represent the virtual obstacles constructed from *quadtree* partitioning. The thin black line with the green arrows contained in thin black circle is the Dubin's car optimized trajectory. The heat map represents the pressure distribution in term of SPL.

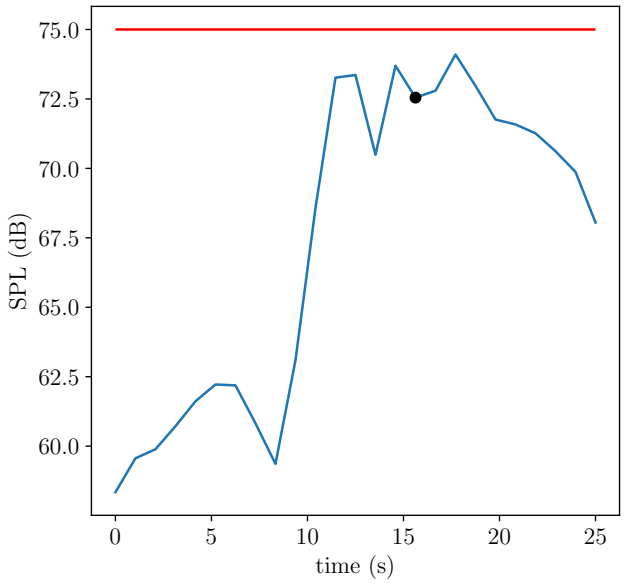

Fig. 3. SPL of the Dubin's car at receiver location for the optimized trajectory. The horizontal red line represents the maximum admissible acoustic noise at 75 dB. The black dot corresponds to the SPL of the discretized trajectory points used to illustrate the exclusion zone in Fig. 2.

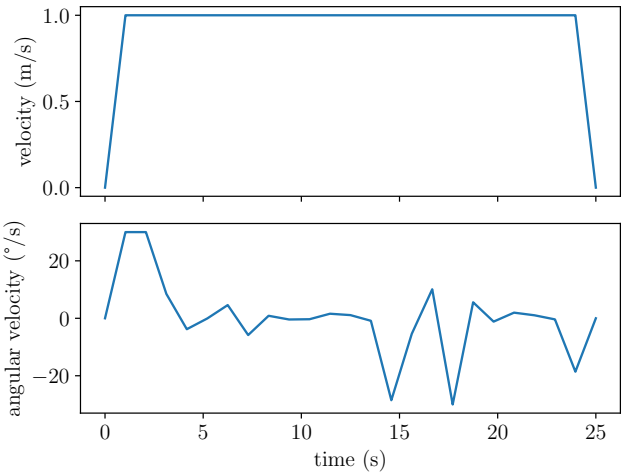

Fig. 4. System control inputs of the generated trajectory. At the top, the evolution of the control u_1 and at the bottom, the control u_2.

multiple non-collision constraints with generic (convex) geometries. However, depending on the maximum depth level, the exclusion zone can be more or less overestimated as seen in Figs. 2 and 3.

In the present study, the exclusion zones were chosen to depend on the control inputs leading to higher computing needs but more realistic results. One can define the worst case scenario and use a constant acoustic exclusion zone for all possible control inputs. This method can be very fast, but it overestimates the solution, which limits flexibility.

In addition, acoustic computation using BEM can only be done for a single value of the wave number k at once. Additional computations need to be performed if multiple frequencies exist in the frequency band of the acoustic source. The use of parallel computing is appreciated as it can radically speed up the overall computation time. The controls are assumed to be piecewise constant, transitional regimes are not considered here. As each discretization point is considered acoustically independent (steady state condition for each control), the BEM can be computed in parallel. The current study was conducted in 2D, and slight modifications to the overall problem are required for 3D computations. While this will increase computational costs, the problem formulation itself will only be impacted by the change in dimensionality or the expression of equations in 3D instead of 2D.

Future work

The current algorithm was implemented using the high-level programming language *Python* as a proof of concept. Significant improvements in computation time could be achieved by transitioning to compiled languages such as *C* or *C++*.

In addition, some issues arise when the constraints are sequentially updated. Externalized BEM computations in the iteration sequence of SCvx are used to update the virtual obstacles according to the last control inputs. Hence, the current local subproblem constraints depend on the previous values of the controls. As no gradient-based information is used, the algorithm may take a longer time to converge toward the best direction. Special attention will be given to this aspect to improve the algorithm performances and the "dynamic" aspect of the virtual obstacles.

To demonstrate the applicability of this method, future studies will focus on 3D problems involving multiple physical obstacles. Additional features, such as source directivity, may also be incorporated.

VI. Conclusion

The current paper proposed a reformulation of an OCP including acoustic constraints using the ART. The reformulated problem facilitates the generation of acoustically aware trajectories by employing state-of-the-art methods to achieve efficient optimization. The ART allows the generation of virtual obstacles representing acoustic constraints and transforms the original problem into a collision-free trajectory planning problem. The BEM offers a cost-effective solution for simulating acoustic propagation in exterior environments and addressing sound scattering problems. Sequential programming-based methods externalizes acoustic simulations and, through SCvx, reduces the complexity of the problem.

The proposed contribution was demonstrated using a proof of concept implementation with a classical toy example. The strength resides in the virtual obstacles construction. Indeed, as they can be considered as obstacle avoidance constraints, gradients of the BEM formulations are not needed.

This work investigated the main aspects of path planning problem with acoustic constraints. Although the focus was on exterior and sound scattering problems, the approach is not limited to these issues. As discussed in the previous section, numerous additional considerations can be taken into account for further developments.

References

[1] F. Gul, W. Rahiman, and S. S. Nazli Alhady, "A comprehensive study for robot navigation techniques," *Cogent Engineering*, vol. 6, no. 1, p. 1632046, 2019.

[2] L. Liu, X. Wang, X. Yang, H. Liu, J. Li, and P. Wang, "Path planning techniques for mobile robots: Review and prospect," *Expert Systems with Applications*, vol. 227, p. 120254, 2023.

[3] H. Wei and Y. Shi, "MPC-based motion planning and control enables smarter and safer autonomous marine vehicles: Perspectives and a tutorial survey," *IEEE/CAA Journal of Automatica Sinica*, vol. 10, no. 1, pp. 8–24, 2022.

[4] M. Gerdts and S.-J. Kimmerle, "Numerical optimal control of a coupled ODE-PDE model of a truck with a fluid basin," in *Conference Publications*, vol. 2015, pp. 515–524, Conference Publications, 2015.

[5] P. T. Boggs and J. W. Tolle, "Sequential quadratic programming for large-scale nonlinear optimization," *Journal of computational and applied mathematics*, vol. 124, no. 1-2, pp. 123–137, 2000.

[6] H. Jie, G. Zhu, and W. Hong, "Direct approaches for PDE-constrained dynamic optimization based on space–time orthogonal collocation on finite elements," *Journal of Process Control*, vol. 124, pp. 187–198, 2023.

[7] K. A. Ackerman and I. M. Gregory, "Trajectory generation for noise-constrained autonomous flight operations," in *AIAA Scitech 2020 Forum*, p. 0978, 2020.

[8] A. Patterson, K. A. Ackerman, N. Hovakimyan, and I. M. Gregory, "Trajectory generation for distributed electric propulsion vehicles with propeller synchronization," in *AIAA Scitech 2021 Forum*, p. 0586, 2021.

[9] M. B. Galles and B. A. Newman, "Reducing the noise impact of small aircraft through indirect trajectory optimization," in *AIAA Aviation 2020 Forum*, p. 2594, 2020.

[10] P. Dieumegard, F. Guntzer, J. Caillet, and S. Cafieri, "A realistic rotorcraft noise footprint computation for low-noise trajectory optimization," in *78th Vertical Flight Society Annual Forum*, 2022.

[11] K. A. Ackerman and I. M. Gregory, "Comparison of acoustic models and trajectory generation methods for an acoustically-aware aircraft," in *AIAA Scitech 2023 Forum*, p. 2543, 2023.

[12] R. Adlakha, W. Liu, S. Chowdhury, M. Zheng, and M. Nouh, "Integration of acoustic compliance and noise mitigation in path planning for drones in human–robot collaborative environments," *Journal of Vibration and Control*, vol. 29, no. 19-20, pp. 4757–4771, 2023.

[13] L. L. Thompson, "A review of finite-element methods for time-harmonic acoustics," *The Journal of the Acoustical Society of America*, vol. 119, no. 3, pp. 1315–1330, 2006.

[14] J. T. Etgen and M. J. O'Brien, "Computational methods for large-scale 3D acoustic finite-difference modeling: A tutorial," *Geophysics*, vol. 72, no. 5, pp. SM223–SM230, 2007.

[15] S. Kirkup, "The boundary element method in acoustics: A survey," *Applied Sciences*, vol. 9, no. 8, p. 1642, 2019.

[16] P. Charalampous and D. Michael, "Sound propagation in 3D spaces using computer graphics techniques," in *2014 International Conference on Virtual Systems & Multimedia (VSMM)*, pp. 43–49, IEEE, 2014.

[17] K. Shigemi, S. Koyama, T. Nakamura, and H. Saruwatari, "Physics-informed convolutional neural network with bicubic spline interpolation for sound field estimation," in *2022 International Workshop on Acoustic Signal Enhancement (IWAENC)*, pp. 1–5, IEEE, 2022.

[18] Z. Gao, A. Porcayo, and J.-P. Clarke, "Developing virtual acoustic terrain for urban air mobility trajectory planning," *Transportation Research Part D: Transport and Environment*, vol. 120, p. 103794, 2023.

[19] L. Rayleigh, "On the application of the principle of reciprocity to acoustics," *Proceedings of the Royal Society of London*, vol. 25, pp. 118–122, 1876.

[20] J. W. Strutt, "Some general theorems relating to vibrations," *Proceedings of the London Mathematical Society*, vol. 1, no. 1, pp. 357–368, 1871.

[21] L. M. Lyamshev, "Theory of sound radiation by thin elastic shells and plates," *Sov. Phys. Acoust,*, vol. 5, no. 4, pp. 431–438, 1960.

[22] P. Samarasinghe, T. D. Abhayapala, and W. Kellermann, "Acoustic reciprocity: An extension to spherical harmonics domain," *The Journal of the acoustical society of America*, vol. 142, no. 4, pp. EL337–EL343, 2017.

[23] Y. Mao, M. Szmuk, and B. Açıkmeşe, "Successive convexification of non-convex optimal control problems and its convergence properties," in *2016 IEEE 55th Conference on Decision and Control (CDC)*, pp. 3636–3641, IEEE, 2016.

[24] S. A. Sauter, C. Schwab, S. A. Sauter, and C. Schwab, *Boundary element methods*. Springer, 2011.

[25] T. Betcke and M. W. Scroggs, "Bempp-cl: A fast Python based just-in-time compiling boundary element library.," *Journal of Open Source Software*, vol. 6, no. 59, p. 2879, 2021.

[26] D. Malyuta, T. P. Reynolds, M. Szmuk, T. Lew, R. Bonalli, M. Pavone, and B. Açıkmeşe, "Convex optimization for trajectory generation: A tutorial on generating dynamically feasible trajectories reliably and efficiently," *IEEE Control Systems Magazine*, vol. 42, no. 5, pp. 40–113, 2022.

[27] D. Ioan, S. Olaru, S.-I. Niculescu, I. Prodan, and F. Stoican, "Navigation in a multi-obstacle environment. from partition of the space to a zonotopic-based MPC," in *2019 18th European Control Conference (ECC)*, pp. 1772–1777, IEEE, 2019.